Simulation of Bipolar Organic Semiconductor Devices based on the Master Equation including Generation and Recombination

Weifeng Zhou, Christoph Zimmermann, Christoph Jungemann
Chair of Electromagnetic Theory
RWTH Aachen University
Aachen 52056, Germany
Email: wz@ithe.rwth-aachen.de

***Abstract*—A new model for the simulation of bipolar organic semiconductor devices by a three-dimensional master equation is proposed. A single-layer diode with a cubic lattice is investigated. Generation and recombination of electrons and holes are included consistently, where a single parameter, the lifetime, controls the rates. Current-voltage characteristics, carrier density and recombination rate profiles of symmetric and asymmetric bipolar devices are presented with Gaussian disorder of hopping site energy levels for electrons and holes.**

I. Introduction

Organic light emitting diodes (OLEDs) generate light through excitonic processes, which result from recombination of injected electrons and holes [1]. Recombination expressions which had been validated by three-dimensional (3-D) bulk Monte-Carlo (MC) simulations [2]–[4] have widely been used in one-dimensional (1-D) drift-diffusion (DD) device simulations, e.g. [5], [6]. Also a few 3-D MC device simulations have been performed [1], [7]. MC simulations, however, are often extremely time-consuming compared to 3-D master equation (ME) simulations. The 3-D ME has been applied to organic materials with only one carrier type involved, e.g. [8]. To our knowledge, however, it has not yet been applied to recombination in disordered organic semiconductors.

In this article, we present simulations of bipolar OLEDs based on the 3-D ME, which has been extensively studied for different device types in recent years and has the advantages of a much higher efficiency compared to the MC method and a closer relation to the underlying physics than the DD model. The unipolar 3-D ME is extended to the bipolar case including generation and recombination (G-R) of electrons and holes as localized processes.

II. Device Model

In a bipolar semiconductor device, electrons and holes can be generated and recombine at any molecular site i and the rates are determined by their respective occupational probabilities, $p_{i,e}$ and $p_{i,h}$, with a generation lifetime τ/c_i and recombination lifetime τ. Thus, the 3-D ME for electrons reads

$$\sum_{j\neq i}\left[p_{i,e}w_{ij,e}(1-p_{j,e})-p_{j,e}w_{ji,e}(1-p_{i,e})\right] + \frac{p_{i,e}p_{i,h}}{\tau}-c_i\frac{(1-p_{i,e})(1-p_{i,h})}{\tau}=0, \tag{1}$$

and for holes accordingly

$$\sum_{j\neq i}\left[p_{i,h}w_{ij,h}(1-p_{j,h})-p_{j,h}w_{ji,h}(1-p_{i,h})\right] + \frac{p_{i,e}p_{i,h}}{\tau}-c_i\frac{(1-p_{i,e})(1-p_{i,h})}{\tau}=0, \tag{2}$$

with $w_{ij,e}$ and $w_{ij,h}$ denoting the Miller-Abrahams (M-A) hopping rates [9] of electrons and holes, respectively, from site i to j:

$$w_{ij,e}=\begin{cases}\nu_{0,e}\exp\left[-2\alpha r_{ij}-\dfrac{E_{j,e}-E_{i,e}}{k_BT}\right], & E_{j,e}\geq E_{i,e},\\ \nu_{0,e}\exp\left[-2\alpha r_{ij}\right], & E_{j,e}<E_{i,e},\end{cases} \tag{3}$$

$$w_{ij,h}=\begin{cases}\nu_{0,h}\exp\left[-2\alpha r_{ij}-\dfrac{E_{j,h}-E_{i,h}}{k_BT}\right], & E_{j,h}\leq E_{i,h},\\ \nu_{0,h}\exp\left[-2\alpha r_{ij}\right], & E_{j,h}>E_{i,h}.\end{cases} \tag{4}$$

$\nu_{0,e}$ and $\nu_{0,h}$ are the respective hopping prefactors, α is a measure for the strength of carrier localization, and r_{ij} the distance between sites i and j. The last two expressions on the left-hand sides of Eq.(1) and (2) describe recombination and generation, respectively. The generation/recombination process must satisfy the principle of detailed balance at equilibrium and, with the assumption of Fermi-Dirac statistics, the coefficient c_i can be calculated

$$c_i=\frac{p_{i,e}p_{i,h}}{(1-p_{i,e})(1-p_{i,h})}=\exp\left(\frac{E_{i,h}-E_{i,e}}{k_BT}\right), \tag{5}$$

which is only related to the difference between the hole and electron energy on site i and does not depend on the local potential.

The site energies are superpositions of intrinsic energies randomly chosen from a Gaussian distribution with a dimensionless disorder parameter $\hat{\sigma}=\sigma/k_BT$, the image potential and the quasi-static potential obtained by a 1-D Poisson equation. More details can be found in [10]. The intrinsic energies are known as lowest unoccupied molecular orbital (LUMO) energies for electrons and highest occupied molecular orbital (HOMO) energies for holes. In our simulations, equal differences between local HOMO and LUMO energies on each site are assumed.

978-1-4673-7860-4/15/$31.00

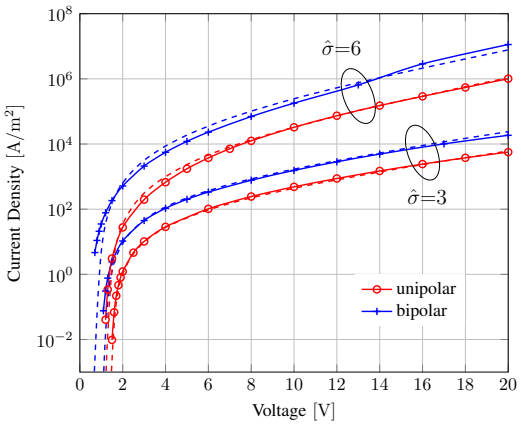

Fig. 1. I-V curves of the unipolar and symmetric bipolar devices using a 3-D ME (symbols and solid lines) and results from [5] (dashed lines) without injection barriers, L=100 nm, a_0=1 nm, Δ=2 eV, T=298 K, α=10^8 cm^{-1}.

TABLE I. HOPPING PREFACTORS AND RECOMBINATION LIFETIMES USED FOR ME SIMULATIONS IN FIG. 1

$\hat{\sigma}$	$\nu_{0,e}(s^{-1})$	$\nu_{0,h}(s^{-1})$	$\tau(s)$
3	2.2×10^{17}	2.2×10^{17}	1×10^{-14}
6	2.2×10^{22}	2.2×10^{22}	1×10^{-25}

The terminal current at the anode of the bipolar device is derived by a Ramo-Shockley-type theorem [10]

$$I_A = C_0\frac{\partial V_A}{\partial t} + \sum_{i,j} q\left[p_{i,h}w_{ij,h}(1-p_{j,h}) - p_{i,e}w_{ij,e}(1-p_{j,e})\right]\frac{x_j - x_i}{L_x}. \quad (6)$$

C_0 is the geometric capacitance and L_x the device thickness. For the stationary case considered here, the first term on the right-hand side of this equation vanishes.

The Newton-Raphson method is used to solve the Poisson equation and the bipolar MEs for electrons and holes self-consistently and a simulation volume with 50×50 sites in the cross-section is investigated below.

III. RESULTS

A. Current of the Symmetric Bipolar Device

The M-A hopping prefactors of unipolar devices with $\hat{\sigma}$=3 and 6 are obtained by matching the corresponding I-V curves calculated by the 1-D continuum model in [5]. Accordingly, the device thickness is L=100 nm, the lattice constant a_0=1 nm, the built-in voltage Δ=2 eV, the temperature T=298 K and the localization parameter α=$10/a_0$. The equal hopping prefactors for electrons and holes, which are listed in Tab. I, are also used to simulate the bipolar symmetric device. With sufficiently short lifetimes (Tab. I), the I-V curves of the bipolar device are comparable to the results in [5], which are based on MC simulations (Fig. 1).

It is well known that low recombination rates lead to very high recombination-limited currents and high recombination rates lead to much lower space-charge-limited currents (see e.g. [11]). The transition between these regimes in our simulations

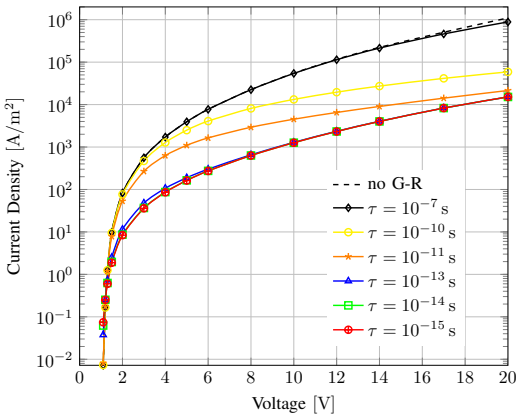

Fig. 2. Simulated I-V curves of bipolar symmetric diodes, excluding (dashed) and including (solid) G-R with various lifetimes and $\hat{\sigma}$=3.

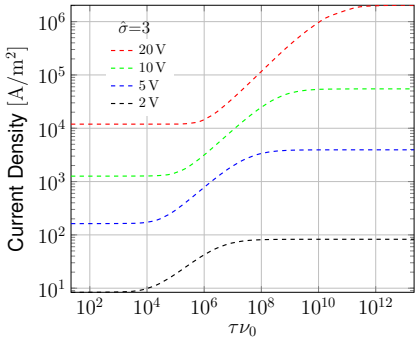

(a)

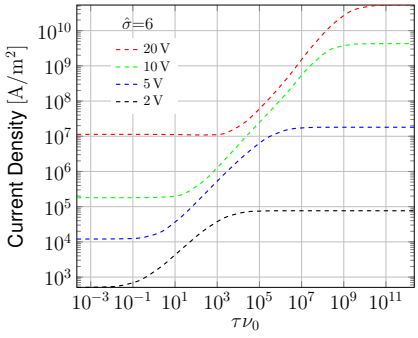

(b)

Fig. 3. Current density in bipolar devices as functions of $\tau\nu_0$ for different voltages and disorder parameters.

is illustrated in Fig. 2. For a sufficiently low value of τ, the I-V curves do not change anymore with further reduction of this value.

To show the influence of τ more clearly, current densities for given voltages are plotted as functions of the product $\tau\nu_0$ (ν_0=$\nu_{0,e}$=$\nu_{0,h}$) for $\hat{\sigma}$=3 and 6 in Fig. 3(a) and 3(b), respectively. It can be seen in Tab. I that the products $\tau\nu_0$ for our simulations in Fig. 1 are always at the low end of the range in Fig. 2. This agrees well with the fact that our simulations match existing results based on MC simulations, which assumed instantaneous recombination on each site.

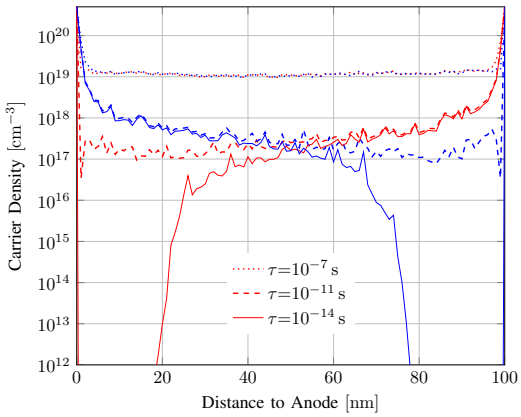

Fig. 4. Spatial distributions of average carrier densities of electrons (red) and holes (blue) with various lifetimes and $\hat{\sigma}$=3 at a voltage of 20 V.

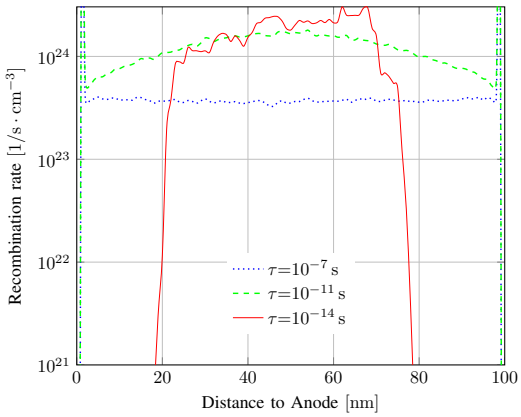

Fig. 5. Spatial distributions of average recombination rates with different lifetimes and $\hat{\sigma}$=3 at a voltage of 20 V.

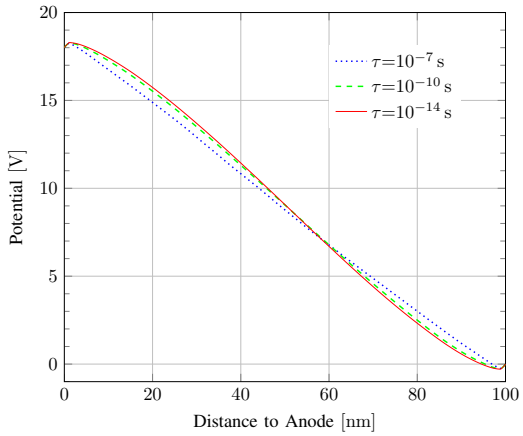

Fig. 6. Quasi-static potential profiles with various lifetimes and $\hat{\sigma}$=3 at a voltage of 20 V.

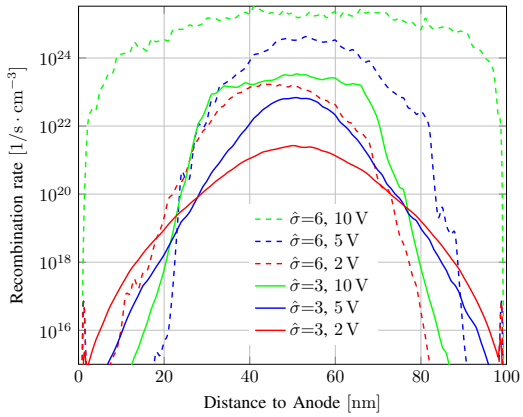

Fig. 7. Spatial distributions of average recombination rates with τ=10^{-14} s for $\hat{\sigma}$=3 (solid) and τ=10^{-25} s for $\hat{\sigma}$=6 (dashed) at various voltages.

B. Carrier Density and Recombination Profile

Average carrier densities in each plane perpendicular to the transport direction are plotted in Fig. 4. For τ=10^{-7} s, recombination is so weak that electrons and holes move freely to their respective collecting electrodes. For shorter lifetimes, electrons (holes) become minorities when approaching the anode (cathode) because of the strong recombination in the center of the device (Fig. 5). The shorter the lifetime, the more pronounced is the confinement of the recombination zone. With stronger recombination, the overlap of electron and hole densities tends to be reduced, which makes the quasi-static potential profile (Fig. 6) more nonlinear. Generation rates are much smaller than recombination rates at forward bias and thus not shown here.

The spatial distributions of the average recombination rates at different voltages with $\hat{\sigma}$=3 and 6 are plotted in Fig. 7 for comparison. Under high bias, the recombination peak turns out to be more broadened with higher disorder energy, which is probably due to the stronger field dependence of the mobility [8].

C. Asymmetric Bipolar Simulations

In real devices, the mobilities of electrons and holes are not the same. Therefore, we also performed simulations of devices being asymmetric with respect to carrier mobilities.

The ratio of hopping prefactors is defined as $\Gamma=\nu_{0,e}/\nu_{0,h}$, with $\nu_{0,e}$ being varied and $\nu_{0,h}$ remaining identical to its value in Tab. I. All other parameters are the same as those in Fig. 1. The distributions of carrier densities at 20 V are plotted in Fig. 8(a) and 8(b) with $\hat{\sigma}$=3 and 6, respectively, for two cases of Γ=0.1 and Γ=0.5. When Γ becomes smaller, more holes are able to move closer to the cathode due to their larger hopping rates and fewer electrons can arrive at the anode.

The recombination profiles similar to Fig. 7 are shown in Fig. 9(a) and 9(b), with $\hat{\sigma}$=3 and 6, respectively. When the value of Γ is reduced, the position of the recombination peak shifts towards the cathode and it becomes more confined than in the symmetric case.

IV. Conclusion

3-D ME simulations of bipolar organic semiconductor devices have been performed. I-V curves, spatial distributions

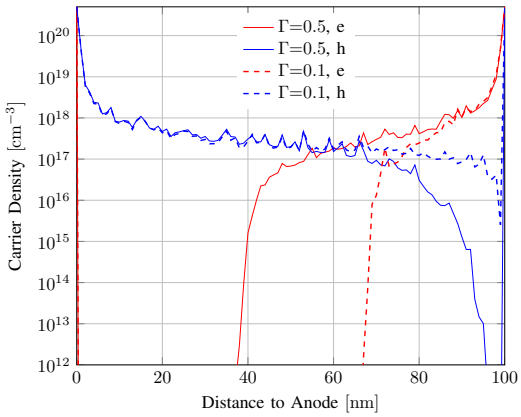

(a)

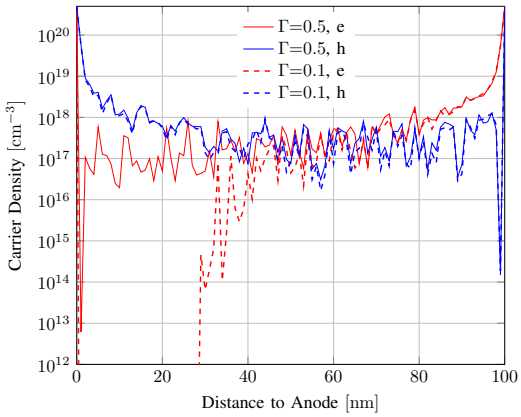

(b)

Fig. 8. Spatial distributions of average carrier densities of electrons (red) and holes (blue) with (a) $\hat{\sigma}$=3 and (b) $\hat{\sigma}$=6 and Γ=0.5 (solid), Γ=0.1 (dashed) at a voltage of 20 V.

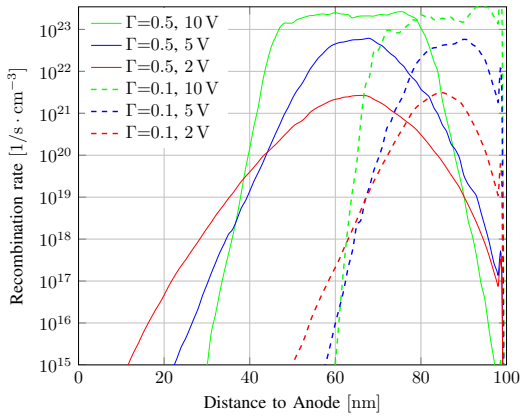

(a)

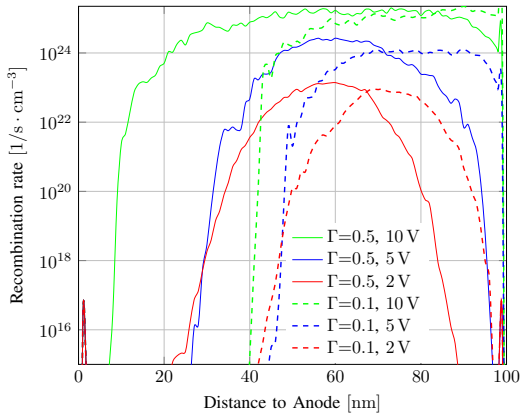

(b)

Fig. 9. Spatial distributions of average recombination rates with (a) $\hat{\sigma}$=3 and (b) $\hat{\sigma}$=6, and Γ=0.5 (solid), 0.1 (dashed) at various voltages.

of carrier densities and recombination profiles have been obtained for different disorder energies. With sufficiently short lifetimes of electron-hole pairs, well-known results from MC simulations can be reproduced, proving the validity of our ME approach. The simulations were also applied to devices with unbalanced carrier mobilities. As expected, the recombination zone of such devices becomes confined close to the electrode injecting the slower carrier type. Our results indicate the potential of an efficient OLED simulation approach, which is transparently based on the relevant physical processes.

References

[1] H. van Eersel, P. A. Bobbert, R. A. J. Janssen and R. Coehoorn, "Monte Carlo study of efficiency roll-off of phosphorescent organic light-emitting diodes: Evidence for dominant role of triplet-polaron quenching," *Appl. Phys. Lett.*, vol. 105, no. 143303, Oct. 2014.

[2] U. Albrecht and H. Baessler, "Langevin-type charge carrier recombination in a disordered hopping system," *Phys. Stat. Sol.*, vol. 191, pp. 455, 1995.

[3] C. Groves and N. C. Greenham, "Bimolecular recombination in polymer electronic devices," *Phys. Rev. B*, vol. 78, no. 155205, Oct. 2008.

[4] J. J. M. van der Holst, F. W. A. van Oost, R. Coehoorn and P. A. Bobbert, "Electron-hole recombination in disordered organic semiconductors: validity of the Langevin formular," *Phys. Rev. B*, vol. 80, no. 235202, Dec. 2009.

[5] R. Coehoorn and S. L. M. van Mensfoort, "Effects of disorder on the current density and recombination profile in organic light-emitting diodes," *Phys. Rev. B*, vol. 80, no. 085302, Aug. 2009.

[6] E. Knapp, R. Haeusermann, H. U. Schwarzenbach and B. Ruhstaller, "Numerical simulation of charge transport in disordered organic semiconductor devices," *J. Appl. Phys.*, vol. 108, no. 054504, 2010.

[7] M. Mesta, M. Carvelli, R. J. de Vries, H. van Eersel, J. J. M. van der Holst, M. Schober, M. Furno, B. Luessem, K. Leo, P. Loebl, R. Coehoorn and P. A. Bobbert, "Molecular-scale simulation of electroluminescence in a multilayer white organic light-emitting diode," *Nat. Mater.*, vol. 12, pp. 652, Apr. 2013.

[8] W. F. Pasveer, J. Cottaar, C. Tanase, R. Coehoorn, P. A. Bobbert, P. W. M. Blom, D. M. de Leeuw and M. A. J. Michels, "Unified description of charge-carrier mobilities in disordered semiconducting polymers," *Phys. Rev. Lett.*, vol. 94, no. 206601, May 2005.

[9] A. Miller and E. Abrahams, "Impurity conduction at low concentrations," *Phys. Rev.*, vol. 120, no. 3, pp. 745, Nov. 1960.

[10] C. Jungemann, "Simulation of electronic noise in disordered organic semiconductor devices based on the master equation," *J. Comp. Elec.*, vol. 14, iss. 1, pp. 37, Mar. 2015.

[11] H. C. F. Martens, W. F. Pasveer, H. B. Brom, J. N. Huiberts and P. W. M. Blom, "Crossover from space-charge-limited to recombination-limited transport in polymer light-emitting diodes," *Phys. Rev. B*, vol. 63, no. 125328, Mar. 2001.